

Reconfigurable terahertz quarter-wave plate for helicity switching based on Babinet inversion of anisotropic checkerboard metasurface

Yosuke Nakata,^{1,*} Kai Fukawa,² Toshihiro Nakanishi,³ Yoshiro Urade,⁴ Kunio Okimura,⁵ and Fumiaki Miyamaru^{2,6}

¹Research Center for Advanced Science and Technology,
The University of Tokyo, 4-6-1 Komaba, Meguro-ku, Tokyo 153-8904, Japan

²Department of Physics, Faculty of Science, Shinshu University,
3-1-1 Asahi, Matsumoto, Nagano 390-8621, Japan

³Department of Electronic Science and Engineering, Kyoto University, Kyoto 615-8510, Japan

⁴Center for Emergent Matter Science, RIKEN, 2-1 Hirosawa, Wako, Saitama 351-0198 Japan

⁵School of Engineering, Tokai University, 4-1-1 Kitakaname, Hiratsuka, Kanagawa 259-1292, Japan

⁶Center for Energy and Environmental Science, Shinshu University, 4-17-1 Wakasato, Nagano 380-8553, Japan

(Dated: Compiled March 23, 2022)

Dynamic helicity switching by utilizing metasurfaces is challenging because it requires deep modulation of polarization states. To realize such helicity switching, this paper proposes a dynamic metasurface functioning as a switchable quarter-wave plate, the fast axis of which can be dynamically rotated by 90° . The device is based on the critical transition of an anisotropic metallic checkerboard, which realizes the deep modulation and simultaneous design of the switchable states. After verifying the functionality of the ideally designed device in a simulation, we tune its structural parameters to realize practical experiments in the terahertz frequency range. By evaluating the fabricated sample with vanadium dioxide, the conductivity of which can be controlled by temperature, its dynamic helicity switching function is demonstrated.

I. INTRODUCTION

Dynamic polarization control technology has been fundamental for flat-panel displays, polarization-sensitive spectroscopy, highly sensitive measurements with the lock-in detection technique, and data transmission. In the optical frequency domain, liquid-crystal and electro-optic-crystal modulators have been widely used to achieve dynamic polarization modulation. However, in lower frequency ranges such as the terahertz frequency range [1], which is potentially important for spectrally resolving giant and bio-molecules, the wavelength is several orders of magnitude larger than that in the optical frequency range. Thus, the thickness of conventional dielectric devices at terahertz frequencies must become much larger than that at optical frequencies, and it is difficult to reach subwavelength-order dynamic devices.

To overcome this difficulty, researchers have been developing artificially designed surfaces, called *metasurfaces* [2–4]. Most metasurfaces are partially made of metals, the highly conductive nature of which is applicable to subwavelength devices. Recently, the progress of metasurfaces has motivated research into dynamic terahertz polarization control utilizing photoswitchable chiral metamolecules [5], deformable MEMS (micro electro mechanical systems) spirals [6, 7], gate-tunable polarization modulators with graphene [8], tunable MEMS cross-polarization converters [9], and tunable wave plates with actuated microcantilever arrays to switch circular and linear polarization states of transmitted waves [10]. Phase change materials such as vanadium dioxide have also been applied to dynamic quarter-wave

plates with variable working frequencies [11, 12] and reconfigurable polarization modulators between linear and circular polarization states [13, 14]. Despite these remarkable achievements, designing switchable metasurfaces that have desired functionalities with deep modulation contrast is still challenging. This is because it also requires the simultaneous design to realize multiple functionalities, which usually interfere with each other.

To resolve this issue, an extremely thin metallic

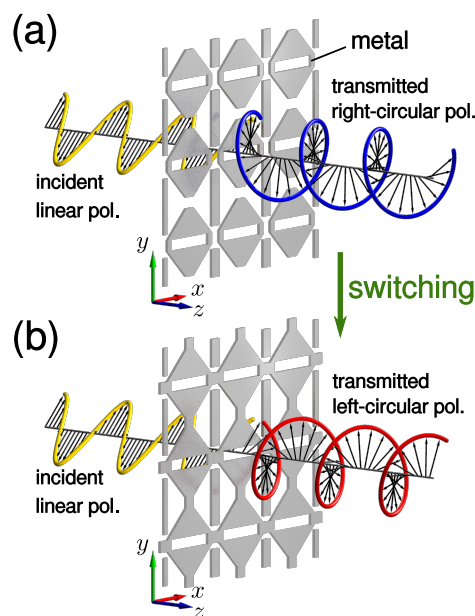


FIG. 1. Schematics for dynamic helicity switching for the transmitted wave by utilizing the transition between the (a) disconnected and (b) connected anisotropic checkerboards.

* nakata@qc.rcast.u-tokyo.ac.jp

checkerboard can be a key structure. The electromagnetic properties of metallic checkerboards critically depend on their connection states [15–19]. Between the connected and disconnected states, extraordinary frequency-independent characteristics have been revealed for the metallic checkerboards with resistive and random connections [20–23]. The checkerboard critical behavior is closely related to the checkerboard special property: the *local* electrical conductivity switching at the interconnection points results in *global* Babinet inversion, which is the generalization of the interchange between the metallic and vacant areas. We can interpret that local conductivity switching can induce a global *phase transition*, which exhibits critical changes in the electromagnetic scattering property. This transition is preferable to realizing not only the deep modulation but also simultaneous design of dynamic metasurfaces, because the original and switched states are related through the structural symmetry of Babinet inversion. This theory has been demonstrated to realize the capacitive-inductive reconfigurable filter [24] and extended to anisotropic checkerboards to realize a reconfigurable polarizer [25]. Even planar chirality switching has been theoretically proposed [26].

In this study, we propose a reconfigurable metasurface based on the anisotropic checkerboard transition to realize helicity switching, which requires the deep modulation and simultaneous design of the switchable states. As shown in Fig. 1, this metasurface converts incident linear polarization to right- or left-circular polarization, depending on the connection states. The device functions as a dynamic quarter-wave plate, the fast axis of which can be rotated by 90° . Compared to a previously studied dynamic polarizer based on an anisotropic checkerboard [25], of which only the amplitude manipulation function was investigated, the dynamic quarter-wave plate requires the simultaneous control of both the amplitude and phase for each polarization. We show that the anisotropic checkerboard can also function as a dynamic quarter-wave plate because of a general constraint between the transmission amplitude and phase, and we demonstrate its functionality in the terahertz frequency range. In this study, we assume a harmonic time dependence $\exp(j\omega t)$, where we use j for the imaginary unit.

II. PRINCIPLE

First, we design an ideal dynamic quarter-wave plate based on the anisotropic checkerboard to demonstrate our strategy for realizing fast axis rotation. Before going into detailed discussion, we explain the general restriction imposed on the complex transmission amplitudes, derived from energy conservation law. Consider a thin electric metasurface located at $z = 0$ in a vacuum. An electromagnetic wave having a complex electric field $\tilde{\mathbf{E}}_0 \exp(-jk_0 z)$ with $k_0 > 0$ enters the metasurface from $z < 0$ to $z > 0$. The transmitted and reflected components propagating along the z -direction with the

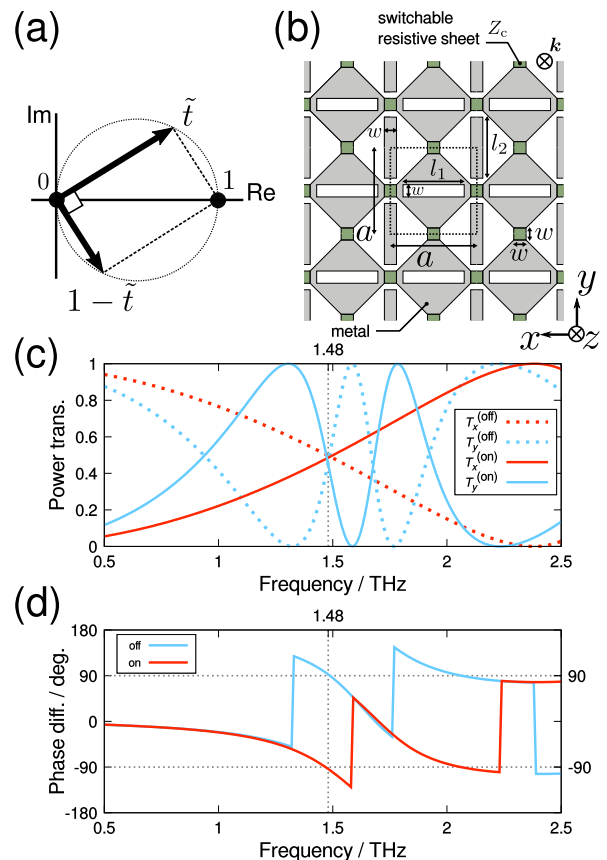


FIG. 2. (a) Constraint on a complex transmission amplitude for lossless electric metasurface without resistive elements, polarization conversion, or diffraction into higher-order modes. (b) Design of a dipole-nested checkerboard metasurface. Calculated (c) power transmission ($T_x = |\tilde{t}_x|^2$, $T_y = |\tilde{t}_y|^2$) and (d) phase difference between transmitted x and y -polarizations [$\arg(\tilde{t}_y) - \arg(\tilde{t}_x)$] for the off- and on-state dipole-nested checkerboard made of perfect metal with $a = 106 \mu\text{m}$, $w = 15 \mu\text{m}$, $l = l_1 = l_2 = 75 \mu\text{m}$ at the normal incidence of plane waves.

same polarization $\tilde{\mathbf{E}}_0$ are denoted by $\tilde{t}\tilde{\mathbf{E}}_0 \exp(-jk_0 z)$ and $\tilde{r}\tilde{\mathbf{E}}_0 \exp(jk_0 z)$, respectively. Here, \tilde{t} (\tilde{r}) is a complex transmission (reflection) coefficient. If there is no energy loss caused by resistive elements, polarization conversion, or diffraction into higher-order modes, the following equation must be satisfied from the electric field continuation $1 + \tilde{r} = \tilde{t}$ at $z = 0$ and energy conservation law $|\tilde{t}|^2 + |\tilde{r}|^2 = 1$:

$$|\tilde{t}|^2 + |1 - \tilde{t}|^2 = 1. \quad (1)$$

This implies that \tilde{t} must be on the circumference of the dashed circle shown in Fig. 2(a). The quarter-wave plate function requires $\tilde{t}_y = \pm j\tilde{t}_x$, where \tilde{t}_i is \tilde{t} for a normally incident i -polarized wave. If we assume Eq. (1) for each polarization, the only possible choice for a quarter-wave plate is $\tilde{t}_x = (1 + j)/2$, $\tilde{t}_y = (1 - j)/2$, or $\tilde{t}_x = (1 - j)/2$, $\tilde{t}_y = (1 + j)/2$ [27, 28]. Under these conditions, $T_x = T_y = 1/2$ is satisfied for the power transmission $T_x = |\tilde{t}_x|^2$,

$$T_y = |\tilde{t}_y|^2.$$

Now, we apply the checkerboard singularity to quarter-wave plate switching. Consider a dipole-nested checkerboard metasurface (D-checkerboard) at $z = 0$ in a vacuum, as shown in Fig. 2(b). The thickness of the metal is safely assumed to be zero if we consider the structure as much thinner than the typical length, such as a . The metasurface is composed of perfectly metallic parts connected with interconnection patches exhibiting variable sheet impedance Z_c . Changing Z_c from ∞ to 0, we can induce the checkerboard transition from the disconnected structure (off state) to the connected structure (on state). The metasurface is designed to be *dynamically Babinet-invertible* for $l = l_1 = l_2$; the on-state structure is obtained by 90° rotation after Babinet inversion of the off-state structure. This special symmetry automatically leads to the transmission inversion for each polarization [25]:

$$\tilde{t}_i^{(\text{off})} + \tilde{t}_i^{(\text{on})} = 1 \quad (i = x, y), \quad (2)$$

where $\tilde{t}_i^{(\text{off})}$ and $\tilde{t}_i^{(\text{on})}$ are \tilde{t}_i for the off and on state checkerboards, respectively. If we assume Eq. (1), the transmission inversion ($\tilde{t}_i^{(\text{off})}$ to $\tilde{t}_i^{(\text{on})} = 1 - \tilde{t}_i^{(\text{off})}$) is represented by 90° rotation in the complex plane, as shown in Fig. 2(a). If we have $\tilde{t}_x^{(\text{off})} = (1 + j)/2$ and $\tilde{t}_y^{(\text{off})} = (1 - j)/2$, then $\tilde{t}_x^{(\text{on})} = (1 - j)/2$ and $\tilde{t}_y^{(\text{on})} = (1 + j)/2$ automatically follow, respectively. Thus, we can realize dynamic rotation of the fast axis of the quarter-wave plate by 90° .

To confirm the above theory, we demonstrate an ideal reconfigurable quarter-wave plate without a substrate, in a simulation. To calculate the transmission spectra of the metasurface in a vacuum, a conventional finite element solver (COMSOL MULTIPHYSICS) was used. All the metal sections are assumed to be perfect electric conductors. Plane waves with x - and y -polarizations normally enter into a metasurface from $z < 0$ to $z > 0$. Using mirror symmetry, the simulation domain is set to a quarter of the unit cell with appropriate side boundary conditions depending on the incident polarization. The top and bottom boundaries are set as ports with only fundamental modes because all calculations are performed under the *diffraction frequency* $f_d = c_0/a = 2.83$ THz (c_0 is the speed of light in a vacuum), above which waves can be diffracted into higher-order modes. Fixing $a = 106 \mu\text{m}$ and $w = 15 \mu\text{m}$, we search the condition to realize $T_x = T_y = 0.5$ by varying $l (= l_1 = l_2)$. Performing parametric sweeps, we found that $T_x = T_y = 0.5$ is realized at 1.48 THz for the off-state structure with $l = 75 \mu\text{m}$. Figure 2(c) presents the power transmission spectra for both the off- and on-state structures with $l = 75 \mu\text{m}$. We can see that the four curves cross at 1.48 THz with a power transmission of 0.5, as we predicted before. Figure 2(d) presents the phase difference $\arg(\tilde{t}_y) - \arg(\tilde{t}_x)$. The phase difference is shifted from $+90^\circ$ to -90° at 1.48 THz for the conductivity switching. These characteristics are guaranteed by transmis-

sion inversion because of the structural symmetry of the anisotropic checkerboard. Thus, we could realize a sub-wavelength terahertz quarter-wave plate, of which the fast axis can be dynamically rotated by 90° .

III. EXPERIMENT WITH OPTIMIZED STRUCTURE

Although the above theoretical consideration works quite well, a substrate is required for a practical device to hold the structures. There is one way to use double-sided substrates sandwiching the structure to assure Babinet inversion [21]. However, we use another approach to slightly modify the structure with a single-sided substrate for simple implementation. In this case, Eq. (2) barely holds, but we can empirically realize quarter-wave plate switching as follows. In the experiments, structures are fabricated on a c -cut sapphire substrate. A vanadium dioxide (VO_2) film grown on the substrate is used as the variable resistance sheets. It exhibits an insulator-to-metal transition of $T_c \approx 340$ K, where the electrical conductivity varies by several orders of magnitude through the transition. To compensate for the substrate effect, we break the symmetry condition $l_1 = l_2$ and tune l_1 and l_2 individually in a simulation to realize quarter-wave plate switching (the other parameters are identical to the previous simulation). The plane wave normally enters into the metasurface at $z = 0$ from a vacuum ($z < 0$) to the sapphire ($z \geq 0$) with refractive index $n_x = n_y = n_\perp \approx 3.1$ and $n_z = n_\parallel \approx 3.4$ [29]. Perfectly matched layer-backed ports are used to calculate spectra above the diffraction frequency $f_d = c_0/(n_\parallel a) = 0.83$ THz. Metallic parts are assumed to be aluminum with a thickness of 400 nm and conductivity $\sigma = 22 \text{ S}/\mu\text{m}$ [30]. The variable resistive connection patch made of VO_2 with a thickness of 200 nm is represented by the sheet impedance of 500 k Ω (off state) and 10 Ω (on state), which are based on DC measurements. The transition boundary condition with the background vacuum permittivity and permeability is imposed onto both the Al and VO_2 parts with their conductivity and thickness. We evaluate the normalized transmission coefficient of the metasurface as $\hat{t}_i = \tilde{t}_i/t_0$, where $t_0 = 2/(1 + n_\perp)$ is the Fresnel coefficient for transmission from a vacuum to the sapphire [31]. To achieve quarter-wave plate switching, we tune l_1 and l_2 as much as possible to realize $\hat{T}_x^{(\text{off})} \approx \hat{T}_y^{(\text{off})} \approx \hat{T}_x^{(\text{on})} \approx \hat{T}_y^{(\text{on})}$ at some frequency, where $\hat{T}_i = |\hat{t}_i|^2$ and on/off represents the connection states. This approximately leads to the switching function. Through the optimization process from $l_1 = l_2 = 75 \mu\text{m}$, we reached $l_1 = 72 \mu\text{m}$ and $l_2 = 76 \mu\text{m}$. The detailed simulation results are presented in Fig. 3.

Using these target parameters, we fabricated a D-checkerboard on a sapphire (0001) substrate (thickness: 1.0 mm). A VO_2 thickness of 200 nm was sputtered and patterned by photolithography using wet etching. The D-checkerboard made of aluminum (thickness: 400 nm)

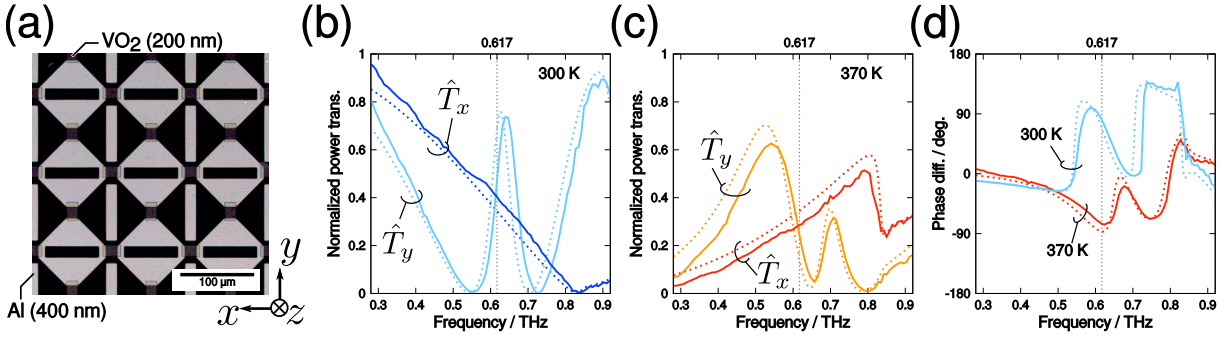


FIG. 3. (a) Microphotograph of the fabricated sample with target lengths $a = 106 \mu\text{m}$, $w = 15 \mu\text{m}$, $l_1 = 72 \mu\text{m}$, and $l_2 = 76 \mu\text{m}$. Normalized power transmission spectra of the sample at (b) 300 and (c) 370 K. (d) Phase difference between transmitted x and y -polarizations for 300 and 370 K. The simulated data (dotted) are also depicted with the experimental data (solid).

was formed by photolithography, electron beam evaporation at room temperature, and the lift-off technique. To ensure electrical connection, the VO_2 squares were partially overlapped by the Al structures. Figure 3(a) presents a top-view microphotograph of the fabricated sample. To evaluate the D-checkerboard, we performed polarization measurements using conventional terahertz time-domain spectroscopy. The sample holder was maintained at 300 and 370 K for the off and on states, respectively. To extend the sample substrate to 3 mm for delaying multiple reflection signals, two pieces of 1 mm-thick c-cut sapphire substrates were placed under the sample. As a reference sample, three stacked pieces of the substrates were used. Multiple reflection signals were truncated using a rectangular time-domain window function. Collimated terahertz waves normally enter into the metasurface. Here, we define $\mathbf{e}_D = (\mathbf{e}_x + \mathbf{e}_y)/\sqrt{2}$ and $\mathbf{e}_X = (-\mathbf{e}_x + \mathbf{e}_y)/\sqrt{2}$, where \mathbf{e}_x and \mathbf{e}_y are the unit vectors along the x and y -axes, respectively. Using wire grid polarizers, we measured \hat{t}_{pq} ($p, q = D, X$), which is a normalized complex transmission amplitude from a normally incident wave with q -polarization into a normally transmitted wave with p -polarization. The normalization is performed through $\tilde{E}_p(\omega)/\tilde{E}_q^{(\text{ref})}(\omega)$, where $\tilde{E}_p(\omega)$ represents the Fourier-transformed transmitted electric field with polarization p for the sample, and $\tilde{E}_q^{(\text{ref})}(\omega)$ is that with polarization q for the reference. After the measurement, we convert \hat{t}_{pq} ($p, q = D, X$) into \hat{t}_{ij} ($i, j = x, y$) using matrix transformation.

Figures 3(b) and (c) present the experimental (solid) and simulated (dotted) data of normalized power transmission spectra $\hat{T}_x = |\hat{t}_x|^2$ and $\hat{T}_y = |\hat{t}_y|^2$ for the off and on states. The experimental data agree quite well with the simulated data. The small discrepancy between the experimental and simulated data is due to the inaccuracy of the fabrication. At 0.617 THz, $\hat{T}_x^{(\text{off})} \approx \hat{T}_y^{(\text{off})} \approx \hat{T}_x^{(\text{on})} \approx \hat{T}_y^{(\text{on})}$ is satisfied. In Fig. 3(d), the phase difference $\arg(\hat{t}_y) - \arg(\hat{t}_x)$ is depicted. Phase difference switching from about $+90^\circ$ to -90° is observed at 0.617 THz. This implies that we have realized fast axis rotation of the quarter-wave plate by 90° . The maximum

device thickness without the substrate is 600 nm, which is deeply subwavelength at the working frequency.

To apply this functionality to the helicity switching of a circular polarization, the polarization of the transmitted wave was analyzed for a normally incident wave with D -polarization. Here, we evaluate S_3/S_0 with the Stokes parameters S_3 and S_0 [32], where $S_3/S_0 = 2\text{Im}(\hat{t}_{xD}^* \hat{t}_{yD}) / (|\hat{t}_{xD}|^2 + |\hat{t}_{yD}|^2)$ represents the z -coordinate in the Poincaré sphere. The right and left circularly polarized waves correspond to $S_3/S_0 = +1, -1$, respectively. Figure 4 presents the S_3/S_0 of the transmitted wave. The helicity of the transmitted wave is dynamically switched at 0.617 THz from $S_3/S_0 = 0.95$ to -0.94 in the experiment.

IV. CONCLUSIONS

We have proposed a terahertz metasurface functioning as a reconfigurable quarter-wave plate, of which the fast axis can be dynamically rotated by 90° . The device is

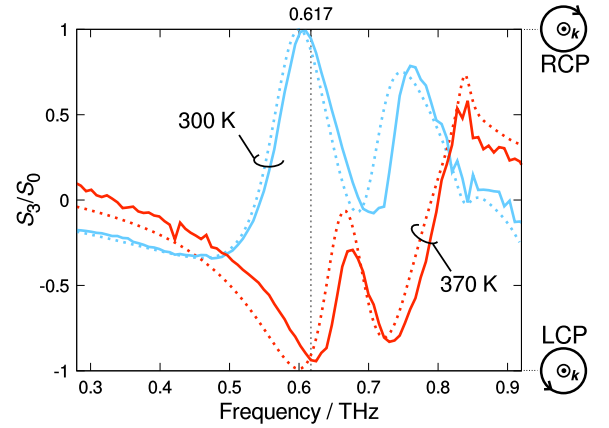


FIG. 4. S_3/S_0 of the transmitted wave for a normally incident plane wave with D -polarization under 300 and 370 K. The simulated data (dotted) are also depicted with the experimental data (solid).

based on the checkerboard critical transition, which realizes the deep modulation and simultaneous design of the off and on states of the device. Combining the constraint on complex transmission amplitudes with transmission inversion, we theoretically showed that 90° fast axis rotation can be realized. Performing simulations for the ideal structure without a substrate, we confirmed that the theory works well. To compensate the substrate effect for realizing practical experiments, we adjusted the structural parameters by slightly breaking the structural symmetry on the interchange of the metallic and vacant area. The optimized D-checkerboard was fabricated and evaluated in the terahertz range. The experimental data agreed very well with the simulated data, and the fast axis rotation of the quarter-wave plate was realized at 0.617 THz. By analyzing the polarization of the transmitted wave for a normally incident D -polarization wave, we demonstrated the helicity switching function of the device. This device is applicable to chirality-sensitive spectroscopy for materials with circular dichroism and optical activity, highly sensitive measurements, and data transmission with circular polarization. The demonstrated device was practically designed with deeply subwavelength structures on thick substrates to truncate multiple reflec-

tion signals. For more efficient devices, we should further consider the elimination of multiple reflections by using a thinner substrate or anti-reflecting coating at the backside of the substrate. The proposed design strategy to realize the reconfigurable quarter-wave plate is not limited to the terahertz frequency range; it is applicable to other frequency ranges, where variable resistance materials can be used. By utilizing photo-carrier injection into semiconductors, ultrafast polarization control can be achieved. Broadband switching should also be studied in the future, although subwavelength devices commonly require resonant behavior, which leads to narrowband operation.

ACKNOWLEDGMENT

The sample fabrication was performed with the help of the Kyoto University Nano Technology Hub, as part of the Nanotechnology Platform Project, sponsored by MEXT, Japan. The present research is supported by a grant from the Murata Science Foundation and by JSPS KAKENHI Grant Nos. 17K17777 and 17K05075.

-
- [1] Y.-S. Lee, *Principles of Terahertz Science and Technology* (Springer, New York, 2009).
- [2] S. B. Glybovski, S. A. Tretyakov, P. A. Belov, Y. S. Kivshar, and C. R. Simovski, Metasurfaces: From microwaves to visible, *Phys. Rep.* **634**, 1 (2016).
- [3] H.-T. Chen, A. J. Taylor, and N. Yu, A review of metasurfaces: physics and applications, *Rep. Prog. Phys.* **79**, 076401 (2016).
- [4] I. Al-Naib and W. Withayachumnankul, Recent progress in terahertz metasurfaces, *J. Infrared, Millimeter, Terahertz Waves* **38**, 1067 (2017).
- [5] S. Zhang, J. Zhou, Y.-S. Park, J. Rho, R. Singh, S. Nam, A. K. Azad, H.-T. Chen, X. Yin, A. J. Taylor, and X. Zhang, Photoinduced handedness switching in terahertz chiral metamolecules, *Nat. Commun.* **3**, 942 (2012).
- [6] T. Kan, A. Isozaki, N. Kanda, N. Nemoto, K. Konishi, M. Kuwata-Gonokami, K. Matsumoto, and I. Shimoyama, Spiral metamaterial for active tuning of optical activity, *Appl. Phys. Lett.* **102**, 221906 (2013).
- [7] T. Kan, A. Isozaki, N. Kanda, N. Nemoto, K. Konishi, H. Takahashi, M. Kuwata-Gonokami, K. Matsumoto, and I. Shimoyama, Enantiomeric switching of chiral metamaterial for terahertz polarization modulation employing vertically deformable MEMS spirals, *Nat. Commun.* **6**, 8422 (2015).
- [8] Z. Miao, Q. Wu, X. Li, Q. He, K. Ding, Z. An, Y. Zhang, and L. Zhou, Widely tunable terahertz phase modulation with gate-controlled graphene metasurfaces, *Phys. Rev. X* **5**, 041027 (2015).
- [9] M. Zhang, W. Zhang, A. Q. Liu, F. C. Li, and C. F. Lan, Tunable polarization conversion and rotation based on a reconfigurable metasurface, *Sci. Rep.* **7**, 12068 (2017).
- [10] X. Zhao, J. Schalch, J. Zhang, H. R. Seren, G. Duan, R. D. Averitt, and X. Zhang, Electromechanically tunable metasurface transmission waveplate at terahertz frequencies, *Optica* **5**, 303 (2018).
- [11] D. Wang, L. Zhang, Y. Gu, M. Q. Mehmood, Y. Gong, A. Srivastava, L. Jian, T. Venkatesan, C.-W. Qiu, and M. Hong, Switchable ultrathin quarter-wave plate in terahertz using active phase-change metasurface, *Sci. Rep.* **5**, 15020 (2015).
- [12] D. Wang, L. Zhang, Y. Gong, L. Jian, T. Venkatesan, C.-W. Qiu, and M. Hong, Multiband switchable terahertz quarter-wave plates via phase-change metasurfaces, *IEEE Photon. J.* **8**, 5500308 (2016).
- [13] X. Liu, X. Chen, E. P. J. Parrott, C. Han, G. Humbert, A. Crunteanu, and E. Pickwell-MacPherson, Invited article: An active terahertz polarization converter employing vanadium dioxide and a metal wire grating in total internal reflection geometry, *APL Photonics* **3**, 051604 (2018).
- [14] M. T. Nouman, J. H. Hwang, M. Faiyaz, K.-J. Lee, D.-Y. Noh, and J.-H. Jang, Vanadium dioxide based frequency tunable metasurface filters for realizing reconfigurable terahertz optical phase and polarization control, *Opt. Express* **26**, 12922 (2018).
- [15] R. C. Compton, J. C. Macfarlane, L. B. Whitbourn, M. M. Blanco, and R. C. McPhedran, Babinet's principle applied to ideal beam-splitters for submillimetre waves, *Opt. Acta Int. J. Opt.* **31**, 515 (1984).
- [16] K. Kempa, Percolation effects in the checkerboard Babinet series of metamaterial structures, *Phys. Status Solidi Rapid Res. Lett.* **4**, 218 (2010).
- [17] J. D. Edmunds, A. P. Hibbins, J. R. Sambles, and I. J. Youngs, Resonantly inverted microwave transmissivity

- threshold of metal grids, *New J. Phys.* **12**, 063007 (2010).
- [18] K. Takano, F. Miyamaru, K. Akiyama, H. Miyazaki, M. W. Takeda, Y. Abe, Y. Tokuda, H. Ito, and M. Hangyo, Crossover from capacitive to inductive electromagnetic responses in near self-complementary metallic checkerboard patterns, *Opt. Express* **22**, 24787 (2014).
- [19] B. Tremain, C. J. Durrant, I. E. Carter, A. P. Hibbins, and J. R. Sambles, The effect of rotational disorder on the microwave transmission of checkerboard metal square arrays, *Sci. Rep.* **5**, 16608 (2015).
- [20] Y. Nakata, Y. Urade, T. Nakanishi, and M. Kitano, Plane-wave scattering by self-complementary metasurfaces in terms of electromagnetic duality and Babinet's principle, *Phys. Rev. B* **88**, 205138 (2013).
- [21] Y. Urade, Y. Nakata, T. Nakanishi, and M. Kitano, Frequency-independent response of self-complementary checkerboard screens, *Phys. Rev. Lett.* **114**, 237401 (2015).
- [22] Y. Urade, Y. Nakata, T. Nakanishi, and M. Kitano, Broadband and energy-concentrating terahertz coherent perfect absorber based on a self-complementary metasurface, *Opt. Lett.* **41**, 4472 (2016).
- [23] K. Takano, Y. Tanaka, G. Moreno, A. Chahadiah, A. Ghaddar, X.-L. Han, F. Vaurette, Y. Nakata, F. Miyamaru, M. Nakajima, M. Hangyo, and T. Akalin, Energy loss of terahertz electromagnetic waves by nano-sized connections in near-self-complementary metallic checkerboard patterns, *J. Appl. Phys.* **122**, 063101 (2017).
- [24] Y. Urade, Y. Nakata, K. Okimura, T. Nakanishi, F. Miyamaru, M. W. Takeda, and M. Kitano, Dynamically Babinet-invertible metasurface: a capacitive-inductive reconfigurable filter for terahertz waves using vanadium-dioxide metal-insulator transition, *Opt. Express* **24**, 4405 (2016).
- [25] Y. Nakata, Y. Urade, K. Okimura, T. Nakanishi, F. Miyamaru, M. W. Takeda, and M. Kitano, Anisotropic Babinet-invertible metasurfaces to realize transmission-reflection switching for orthogonal polarizations of light, *Phys. Rev. Appl.* **6**, 044022 (2016).
- [26] Y. Urade, Y. Nakata, T. Nakanishi, and M. Kitano, Theoretical study on dynamical planar-chirality switching in checkerboard-like metasurfaces, *EPJ Appl. Metamat.* **4**, 2 (2017).
- [27] J. D. Baena, J. P. del Risco, A. P. Slobozhanyuk, S. B. Glybovski, and P. A. Belov, Self-complementary metasurfaces for linear-to-circular polarization conversion, *Phys. Rev. B* **92**, 245413 (2015).
- [28] J. D. Baena, S. B. Glybovski, J. P. del Risco, A. P. Slobozhanyuk, and P. A. Belov, Broadband and thin linear-to-circular polarizers based on self-complementary zigzag metasurfaces, *IEEE Trans. Antennas Propag.* **65**, 4124 (2017).
- [29] D. Grischkowsky, S. Keiding, M. van Exter, and C. Fattinger, Far-infrared time-domain spectroscopy with terahertz beams of dielectrics and semiconductors, *J. Opt. Soc. Am. B* **7**, 2006 (1990).
- [30] N. Laman and D. Grischkowsky, Terahertz conductivity of thin metal films, *Appl. Phys. Lett.* **93**, 051105 (2008).
- [31] \tilde{t}_i is also defined through the transmitted component $\tilde{t}_i \tilde{\mathbf{E}}_i \exp(-jn_{\perp}k_0z)$ in $z \geq 0$ for the i -polarized incident wave $\tilde{\mathbf{E}}_i \exp(-jk_0z)$ in $z < 0$.
- [32] B. E. A. Saleh and M. C. Teich, *Fundamentals of Photonics* (John Wiley & Sons, Inc., Hoboken, New Jersey, 2007).